Core Planar Cell Polarity Genes *VANGL1* and *VANGL2* in Predisposition to Congenital Vertebral Malformations

SI Appendix file

SI Materials and methods

Skeletal preparation

E17.5–E18.5 mouse embryos were eviscerated, dissected, and fixed in 100% ethanol (EtOH) for 2–3 days. After acetone treatment for 2–3 days, embryos were stained for 2–7 days (depending on the size of the skeleton) at room temperature in 5% glacial acetic acid, 0.015% Alcian Blue 8GX, and 0.005% Alizarin Red S in EtOH. After washing with deionized water, the embryos were transferred to 1% KOH/20% glycerol solution until all non-skeletal tissues were completely cleared. The cleared samples were stored in 100% glycerol for long-term preservation. Images were obtained with a Leica MZ10F Fluorescence Modular Stereo Microscope under a bright field.

Whole-mount immunofluorescence staining

C57BL/6 mouse embryos were dissected in 1X phosphate-buffered saline (PBS) (pH 7.4, 137 mM NaCl, 2.7 mM KCl, 10 mM Na_2HPO_4, 1.8 mM KH_2PO_4), and amniotic membranes were collected for genotyping. After embryos were fixed in 4% paraformaldehyde (PFA)/PBS for 45 min at room temperature, they were permeabilized with 0.5% Triton X-100/PBS for 10 min and washed with 1X PBS for 5 min. The embryos were blocked in blocking solution (2% goat serum and 2% donkey serum in PBST [0.1% Triton X-100/PBS]) overnight at 4°C and then incubated overnight at 4°C in 10% horse serum/PBST with primary antibody (1:100 dilution). After washing 3

times in PBST for 20 min with gentle rocking, embryos were incubated overnight at 4°C in 10% horse serum/PBST with secondary antibody (1:1,000 dilution). After washing 3 times in PBST for 20 min with gentle rocking, embryos were mounted with Molecular Probes™ ProLong™ Diamond Antifade Mountant with DAPI (Thermo Fisher Scientific, #P36971). The following antibodies were used: anti-VANGL1 (Atlas Antibodies #HPA025235), anti-VANGL2 (clone 2G4, Millipore Sigma #MABN750), Alexa Fluor 488 donkey anti-rabbit (Invitrogen # A-21206), and Alexa Fluor 568 goat anti-rat (Invitrogen # A-11077). Z-stack images were obtained with a ZEISS LSM800 microscope.

Whole-mount *in situ* hybridization

E8.5 and E9.5 embryos were collected and fixed in 4% PFA/diethyl polycarbonate (DEPC)-PBS. Riboprobes with antisense sequences were labeled using DIG RNA Labeling Mix (Roche #11277073910) with T3, T7, or SP6 RNA polymerase. Plasmids containing the RNA probes were kindly provided by Mai Har Sham (*Wnt3a*, *Fgf8*, *Dll1*, *Dll3, Hes7, Lfng*), Yingzi Yang (*Tbxt*), Kathryn Song Eng Cheah (*Fgf4, Mesp2* and *Tbx6*), and Yasumasa Bessho (*Uncx4.1*). *In situ* hybridization was performed to detect mRNA expression. After dehydration and rehydration through a methanol/PBST series (PBST, 25, 50, and 75% methanol in PBST), embryos were treated with 10 μg/ml proteinase K in DEPC-PBST at room temperature for 20 min for E8.5 embryos and 30 min for E9.5 embryos. After postfixation for 20 min in 0.2% glutaraldehyde in 4%

PFA/DEPC-PBST, embryos were rinsed with hybridization mix (50% formamide, 5X SSC buffer, 1 mg/mL Torula RNA, 100 μg/mL heparin, 0.1% Tween 20, and 0.1% CHAPS) and incubated with the DIG-labeled RNA probe mix overnight at 65°C. Post-hybridization treatments, including RNase A (Sigma-Aldrich, #R6513, 100ug/ml), were used to remove nonspecific hybrids. AP-anti-DIG antibody (Sigma-Aldrich, #11093274910) and BM-Purple (Sigma-Aldrich, #11442074001) were used to detect the probe. Images were acquired with a Leica MZ10F Fluorescence Modular Stereo Microscope.

Whole-mount immunohistochemistry

Whole-mount immunochemistry was performed as previously described (1). E9.5 embryos were dissected in PBS and fixed immediately in DMSO/30% H_2O_2/MeOH (1:1:1) for 1h on ice, followed by washing with 50 mM NH_4Cl at room temperature and then incubation in TS-PBS (PBS, 10% fetal bovine serum, 1% Triton X-100) for 2.5h at 4°C. The embryos were then subjected to anti-cleaved Notch 1 antibody (Cell Signaling, V1744 #4147), biotinylated goat anti-rabbit IgG antibody (Vector Laboratories, #BA-1000-1.5) and streptavidin-HRP (Thermo Scientific, #21130) overnight successively with a dilution of 1/100 in TS-PBS at 4°C. Finally, 4-chloro-1 naphthol was used as the substrate for color visualization and the reaction was stopped by 4% paraformaldehyde. Pictures were taken by Leica MZ10F Fluorescence Modular Stereo Microscope.

Plasmid construction

Human full-length *VANGL1* and *VANGL2* cDNAs were subcloned into the pcDNA3.1 vector (Invitrogen, #V790-20). A hemagglutinin (HA) epitope (YPYDVPDYA) or FLAG tag (DYKDDDDK) was inserted into the N-terminus of VANGL1 or VANGL2. In addition, the Kozak sequence (GCCACC) was inserted immediately before the ATG start codon to increase the translational efficiency. Variants identified in this study were introduced by site-directed mutagenesis. All expression plasmids were verified by Sanger sequencing.

Immunoblotting

HEK293T and MDCK cells cultured in a 12-well plate with 10% fetal bovine serum (FBS, Gibco™ #10099141)/Dulbecco's Modified Eagle Medium (DMEM, Gibco™ #12800017) were used for Western blot analysis. Cells were transfected with 500 ng plasmid for each condition per well using Lipofectamine 3000. After washing with 1X PBS, cells were lysed with 0.1% NP-40/Tris-buffered saline (TBS) and denatured by boiling in 1X Laemmli buffer. Denatured samples were loaded onto an 8% sodium dodecyl sulfate-polyacrylamide gel electrophoresis (SDS-PAGE) gel. Proteins were transferred to the polyvinylidene difluoride (PVDF) membrane and blocked in 5% bovine serum albumin (BSA)/PBS. The membrane was then incubated with primary antibody overnight at 4°C and secondary antibody for 1 h at room temperature. SuperSignal™ West Femto Maximum Sensitivity Substrate (Thermo Fisher Scientific,

#34096) was used to measure the signals of specific proteins. The primary or secondary antibodies used were as follows at a 1:5,000 dilution: anti-β-actin (Sigma-Aldrich #A5441), anti-Flag (Sigma-Aldrich #F1804), anti-HA (Cell Signaling Technology #3724), anti-rabbit (Invitrogen #31460), and anti-mouse (Sigma #GENA9310-1ML). Band intensities were quantitated using ImageJ and normalized with β-actin.

Immunofluorescence

Lipofectamine 3000 Reagent was used to transfect MDCK cells cultured in 10% FBS (Gibco™ 10099141)/DMEM (Gibco™ 12800017). VANGL1 or VANGL2 expression plasmid (500 ng) was transfected in a 24-well plate per experimental condition. For dominant-negative studies, wild-type VANGL2 and mutant VANGL1 or VANGL2 were co-transfected (ratio = 1:1, 250 ng each). Twenty-four hours after transfection, cells were rinsed with 1X PBS, fixed with 4% PFA/PBS at 4°C for 15 min, and permeabilized with 0.5% Triton X-100/PBS for 5 min. Cells were blocked in 3% BSA/0.1% Triton X-100/PBS for 1 h at room temperature and incubated overnight at 4°C in the same blocking buffer with primary antibody (1:1,000 dilution). After washing with 0.1% Triton X-100/PBS, fluorescent secondary antibodies (1:1,000 dilution) were used to detect the target proteins. An ER staining kit (Abcam #ab139482) was used to detect the ER. The cultured cells were incubated in the ER staining solution for 15 min at 37°C after secondary antibody incubation. The primary antibodies used in immunofluorescence were the same as those used for immunoblotting. The

secondary antibodies were Alexa Fluor 488 donkey anti-rabbit (Invitrogen #A-21206) and Alexa Fluor 568 donkey anti-mouse (Invitrogen #A-10037). Confocal images were acquired with a ZEISS LSM800 microscope. Quantification of the intramembrane signal and total signal was performed using ImageJ as described previously (2) and illustrated in Figure S6.

Zebrafish MO and mRNA microinjection

The *AB* zebrafish strain was used for microinjection. Defined MOs and mRNAs were injected into one-cell stage embryos passing through the yolk. Custom MO was purchased from Gene Tools (MO1-*vangl2*: 5'-GTACTGCGACTCGTTATCCATGTC-3', 8 ng/embryo) (3). mRNAs encoding human wild-type or mutant *VANGL1/2* were produced by the T7 Transcription Kit (Invitrogen™ #AM1344). Because either 120 pg of wild-type *VANGL1* or 80 pg of wild-type *VANGL2* completely rescued the CE defects caused by 8 ng *vangl2* MO, these two doses were used for all rescue experiments using mutant *VANGL* mRNA. Forty-eight hours post fertilization, embryos were collected and quantified using ImageJ, and the body axis was examined to compare the severity of mesoderm development defects among the different experimental groups.

Mouse models

The *Vangl1* and *Vangl2* knockout mouse strains and methods for genotyping have been described previously (4). sgRNA targeting the mouse *Vangl1* p.R258H site was

designed by CHOPCHOP v3 (5'-GAAGCGGGACTCTCCGTCGGTGG-3') (5). Two oligos based on the designed sgRNA sequence were synthesized and used to generate the sgRNA plasmid (5'-TAGGAGCGGGACTCTCCGTCGG-3', 5'-AAACCCGACGGAGAGTCCCGCT-3'). The 200 bp ssDNA for introducing the R258H variant was synthesized as 4 nmol ultramers at Integrated DNA Technologies (5'-

CATCTGTCTTCTAGGGTTATTAGTCATCCTTTCTGCTTACTCCGTGTGCATGC

CCCTTACCTCAAGTGTCCCAAGCTGTAGAAGCGGGACTCTCCATCAGTAGA

G**T**GGACCACCTGCAGGGTGAACATGGGTTGCAGCTGCCTCAGCTCCAGCA

GGACGATGGCAAGGTAGTGGATGAAAAGC-3'). sgRNA was synthesized with a MEGAshortscript™ T7 Kit (Thermo Fisher Scientific, #AM1354) followed by purification with a MEGAclear™ Kit (Thermo Fisher Scientific, #AM1908). The synthesized and purified sgRNA and template ssDNA were electroporated into embryos of C57BL/6 mice together with the Cas9 protein in the Transgenic Core Facility, Center for Comparative Medicine Research at the University of Hong Kong. Sanger sequencing was used to validate the *Vangl1* p.R258H point mutation (Forward: CTCTCGGGACCAAAATTACAAG; Reverse: GTCATCCTTTCTGCTTACTCCG). Verified proband mice with homozygous p.R258H mutations were used for breeding offspring for the experiments. All mice used in this study were maintained on C57BL/6 background. Littermates were used if available, but if one experiment needs multiple

embryos with same genotype, embryos from different mating pairs were grouped for studies and N number was provided.

Micro-computed tomography (micro-CT) analyses

Micro-CT (Bruker SkyScan 1276) was performed on adult mice approximately two months of age after euthanasia by CO_2. High-resolution scans of the whole body, including the entire spine, were captured to reconstruct the 3D structure of each vertebra to decipher the skeletal phenotype (pixel size 40 μm). 3D pictures of the whole body, including anterior–posterior, posterior–anterior, and lateral views, and enlarged pictures of looptail regions were captured by multimodal 3D software based on reconstructed structures.

Hypoxia treatment

A BioSpherix Oxycycler system was used to establish the hypoxia environment. We conducted zero calibration and span calibration for each experiment according to the BioSpherix instructions. The BioSpherix OxyCycler system provided oxygen levels of 7.5% or 8.0%. The oxygen level was reduced to 7.5% or 8.0% from the normal oxygen level for over 20 min before each experiment. Afterward, pregnant mice carrying E9.5 embryos were kept in the chamber for 8 h and then gradually transferred to normal oxygen levels. The pregnant mice were sacrificed when the embryos reached E17.5, and those embryos were collected for skeletal preparations.

References:

1. I. Geffers, K. Serth, G. Chapman, R. Jaekel, K. Schuster-Gossler *et al.*, Divergent functions and distinct localization of the Notch ligands DLL1 and DLL3 in vivo. *J Cell Biol* **178**, 465-476 (2007).
2. W. Yang, L. Garrett, D. Feng, G. Elliott, X. Liu *et al.*, Wnt-induced Vangl2 phosphorylation is dose-dependently required for planar cell polarity in mammalian development. *Cell Res* **27**, 1466-1484 (2017).
3. M. Park, R. T. Moon, The planar cell-polarity gene *stbm* regulates cell behaviour and cell fate in vertebrate embryos. *Nat Cell Biol* **4**, 20-25 (2002).
4. H. Song, J. Hu, W. Chen, G. Elliott, P. Andre *et al.*, Planar cell polarity breaks bilateral symmetry by controlling ciliary positioning. *Nature* **466**, 378-382 (2010).
5. K. Labun, T. G. Montague, M. Krause, Y. N. Torres Cleuren, H. Tjeldnes *et al.*, CHOPCHOP v3: expanding the CRISPR web toolbox beyond genome editing. *Nucleic Acids Res* **47**, W171-174 (2019).

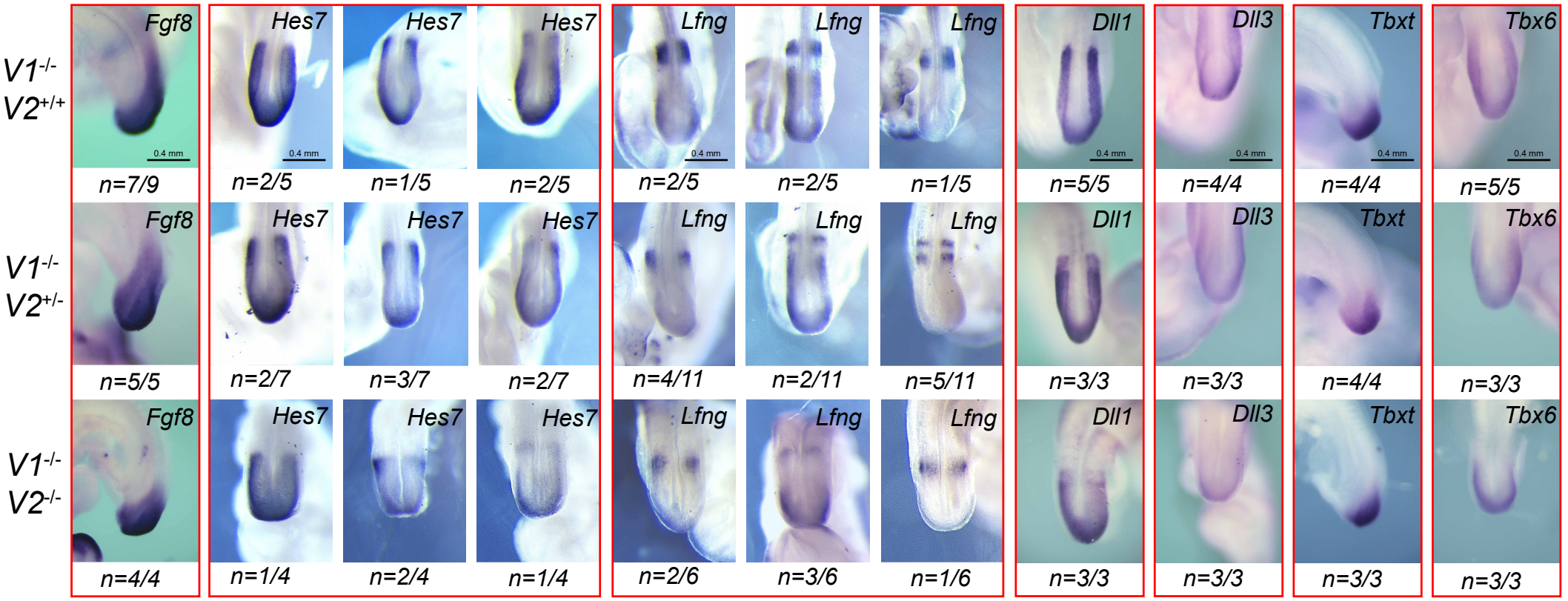

Figure S1. Whole-mount *in situ* hybridizations of somitogenesis markers. Whole-mount *in situ* hybridizations of *Fgf8*, *Hes7*, *Lfng*, *Dll1*, *Dll3*, *Tbxt*, and *Tbx6* in *Vangl1*$^{-/-}$;*Vangl2*$^{+/+}$, *Vangl1*$^{-/-}$;*Vangl2*$^{+/-}$, and *Vangl1*$^{-/-}$;*Vangl2*$^{-/-}$ embryos at E9.5. All the images were captured at the same magnification. V1 denotes *Vangl1* and V2 represents *Vangl2*.

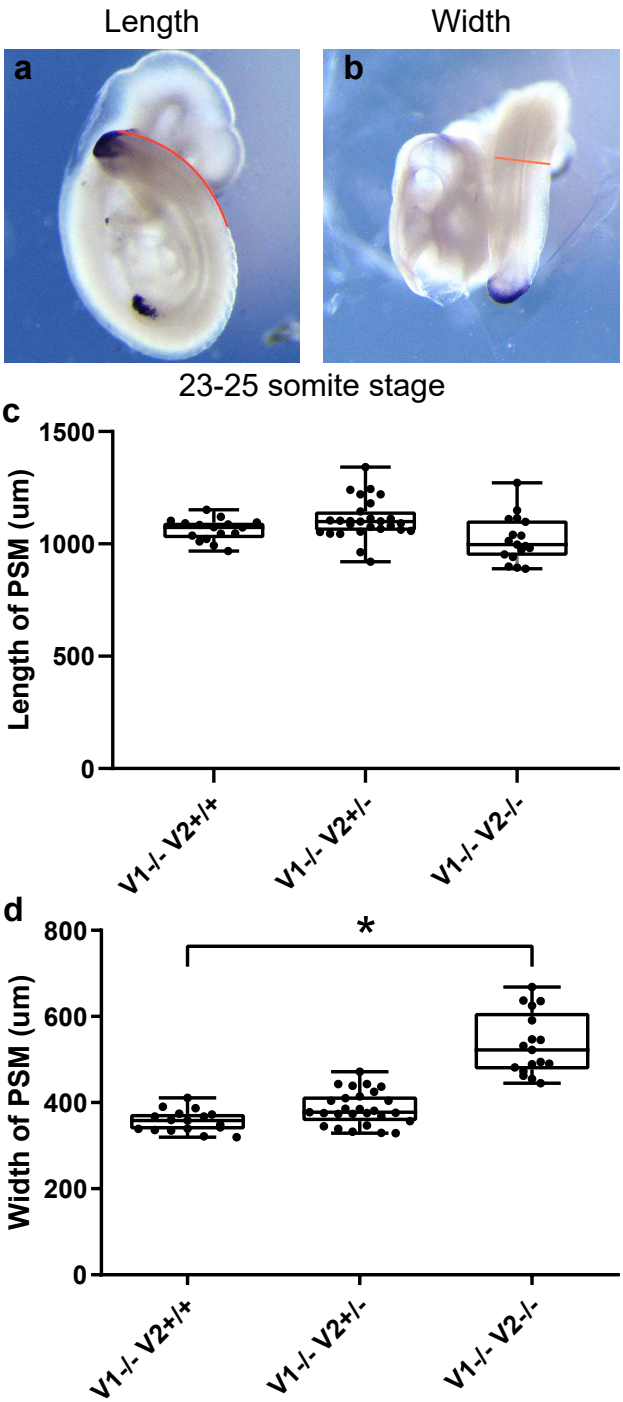

Figure S2. Measurements of PSM length and width in E9.5 embryos in *Vangl1* and *Vangl2* mutant mouse embryos. a The length of the PSM was assessed from the last visible somite to the embryonic posterior end. **b** The width was measured from the left to the right edge underneath the last visible somite. **c** Boxplot of the length of the PSM in three genotypes of *Vangl* mice (*Vangl1*$^{-/-}$;*Vangl2*$^{+/+}$, *Vangl1*$^{-/-}$;*Vangl2*$^{+/-}$, *Vangl1*$^{-/-}$;*Vangl2*$^{-/-}$) in E9.5 embryos at the 23-25 somite stage. **d** Boxplot of the width of the PSM in three genotypes of *Vangl* mice (*Vangl1*$^{-/-}$;*Vangl2*$^{+/+}$, *Vangl1*$^{-/-}$;*Vangl2*$^{+/-}$, *Vangl1*$^{-/-}$;*Vangl2*$^{-/-}$) in E9.5 embryos at the 23-25 somite stage. The statistical significance of differences between the groups was calculated by the one-way ANOVA test, F = 70.70. *p < 0.05. Box plots show center line as median, box limits as upper and lower quartiles, whiskers as minimum to maximum values. V1 denotes *Vangl1* and V2 represents *Vangl2*.

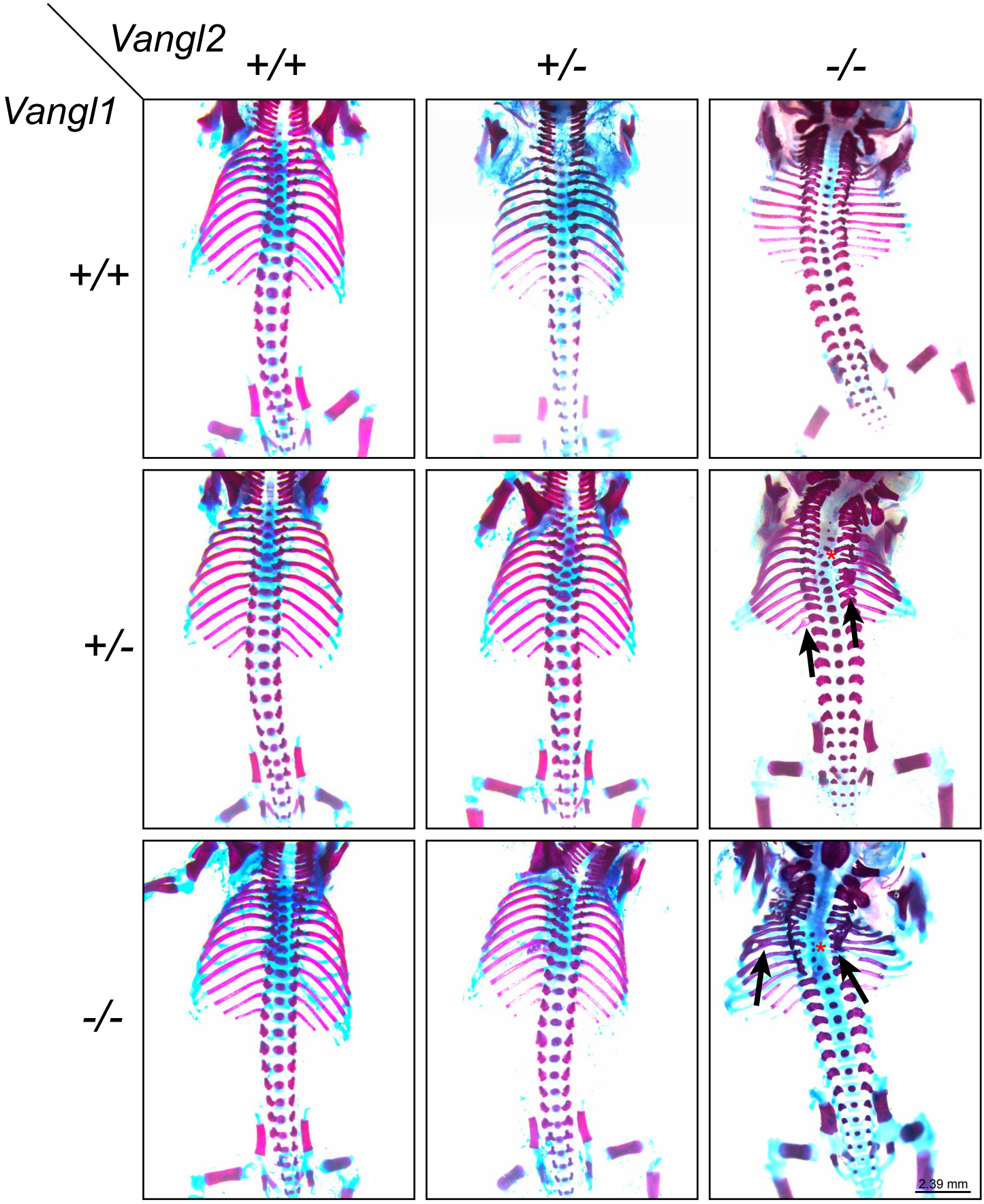

Figure S3. Spinal phenotypes of *Vangl1* and *Vangl2* mutant mice. Skeletal preparation of the E17.5-E18.5 *Vangl1* and *Vangl2* double mutant mouse embryos. Red asterisks indicate vertebral fusion, vertebral misalignment, and delayed vertebral ossification. Arrows denote rib fusion, rib shortening/missing, and rib bifurcation.

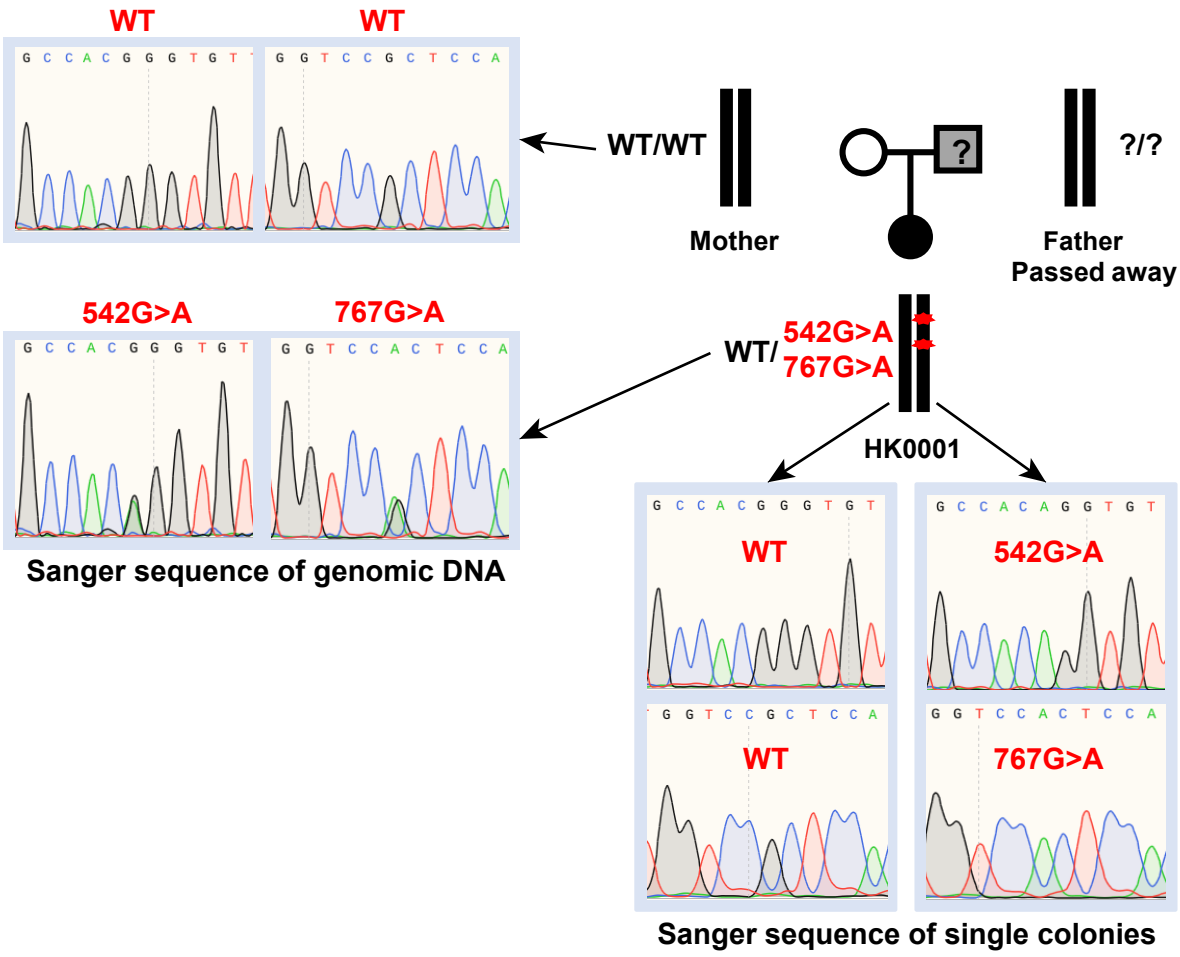

Figure S4. Sanger validation of HK0001 family. *VANGL1* c.542G>A (p.R181Q) and c.767G>A (p.R256H) variants identified in HK0001 family were validated on the same allele by haplotype analysis. *VANGL1* PCR products containing the region of both variants were ligated to plasmid and transformed into bacteria. Single colonies were selected for Sanger Sequencing.

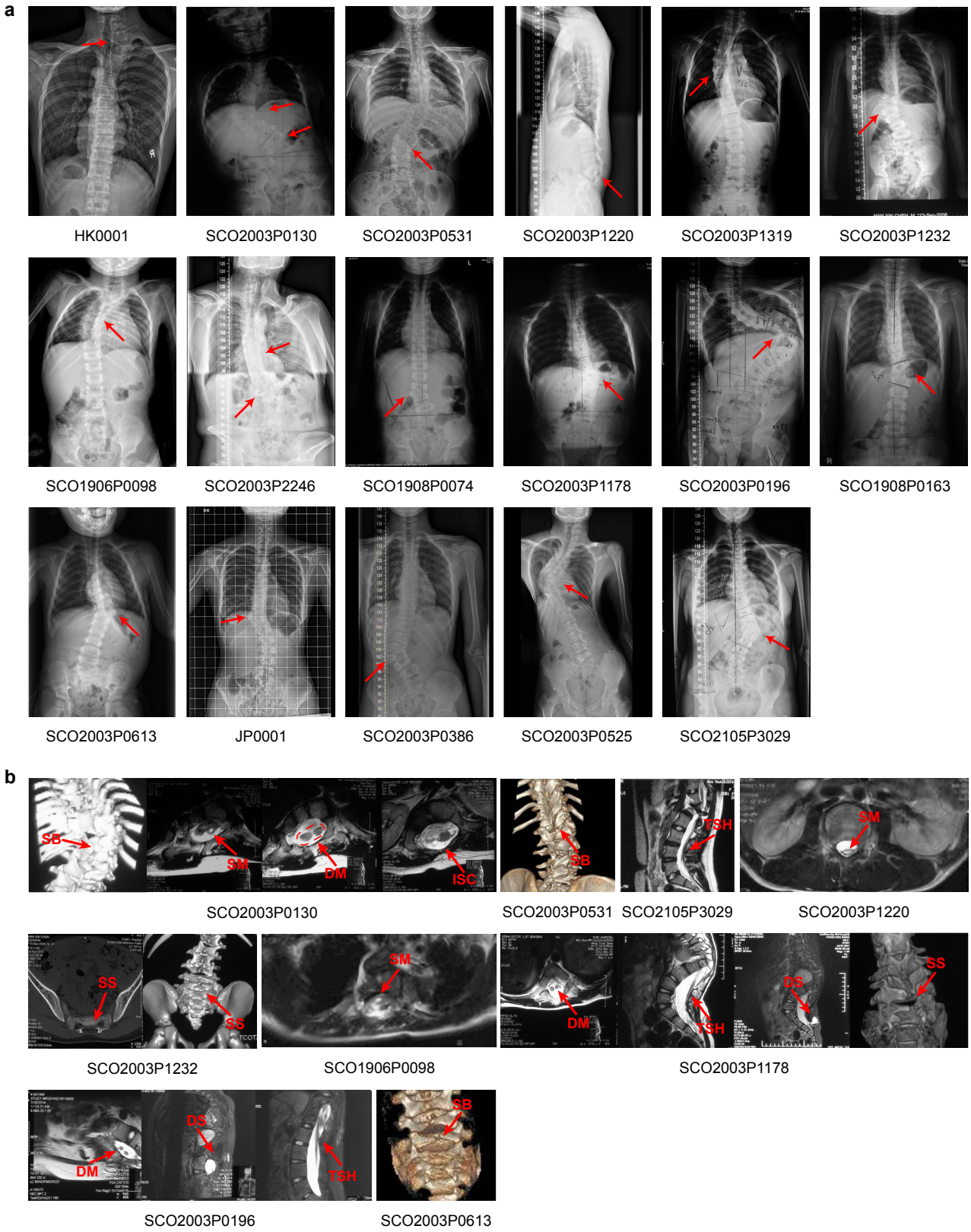

Figure S5. Clinical images of patients with *VANGL1* and *VANGL2* variants. a Spinal X-ray. All patients present different severity of spine deformities, ranging from one vertebral malformation (single-segmented hemivertebrae) to extensive fusion of vertebrae. **b** Intraspinal abnormalities and spinal lamina defects demonstrated by CT or MRI of the spine. Intraspinal abnormalities and spinal lamina defects were commonly seen in CS patients with *VANGL1* and *VANGL2* variants. The vertebral and intraspinal malformations are indicated by red arrows. Abbreviations: SM, syringomyelia; DM, diastematomyelia; ISC, intraspinal cyst; SB, spinal bifida; TSH, tethered spinal cord; SS, sacral schisis; DS, dermal sinus.

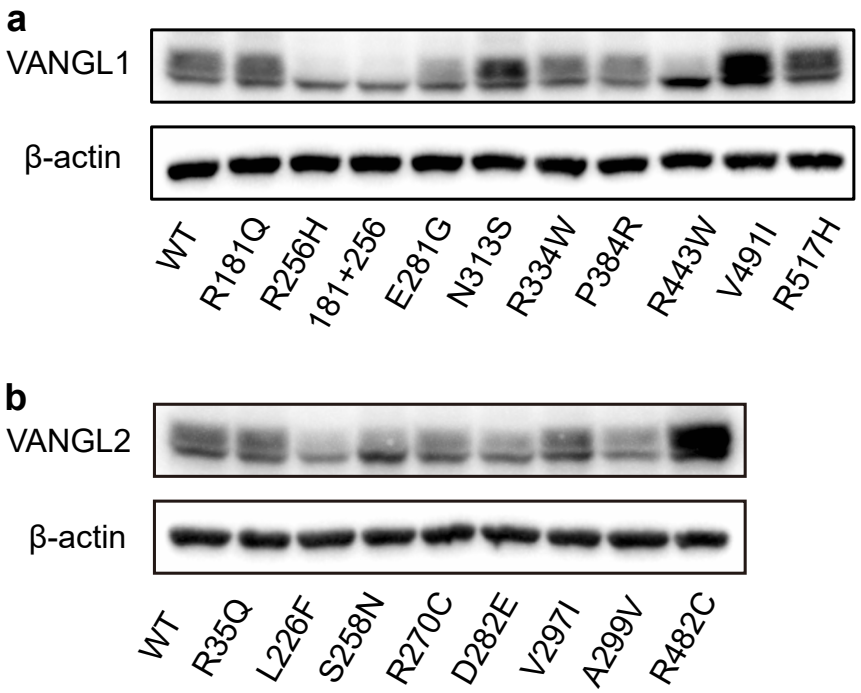

Figure S6. Protein expression of VANGL1 and VANGL2 variants in MDCK cells. a VANGL1; **b** VANGL2. Band intensities of Western blot gels were quantitated using ImageJ, with β-actin used as an internal loading control.

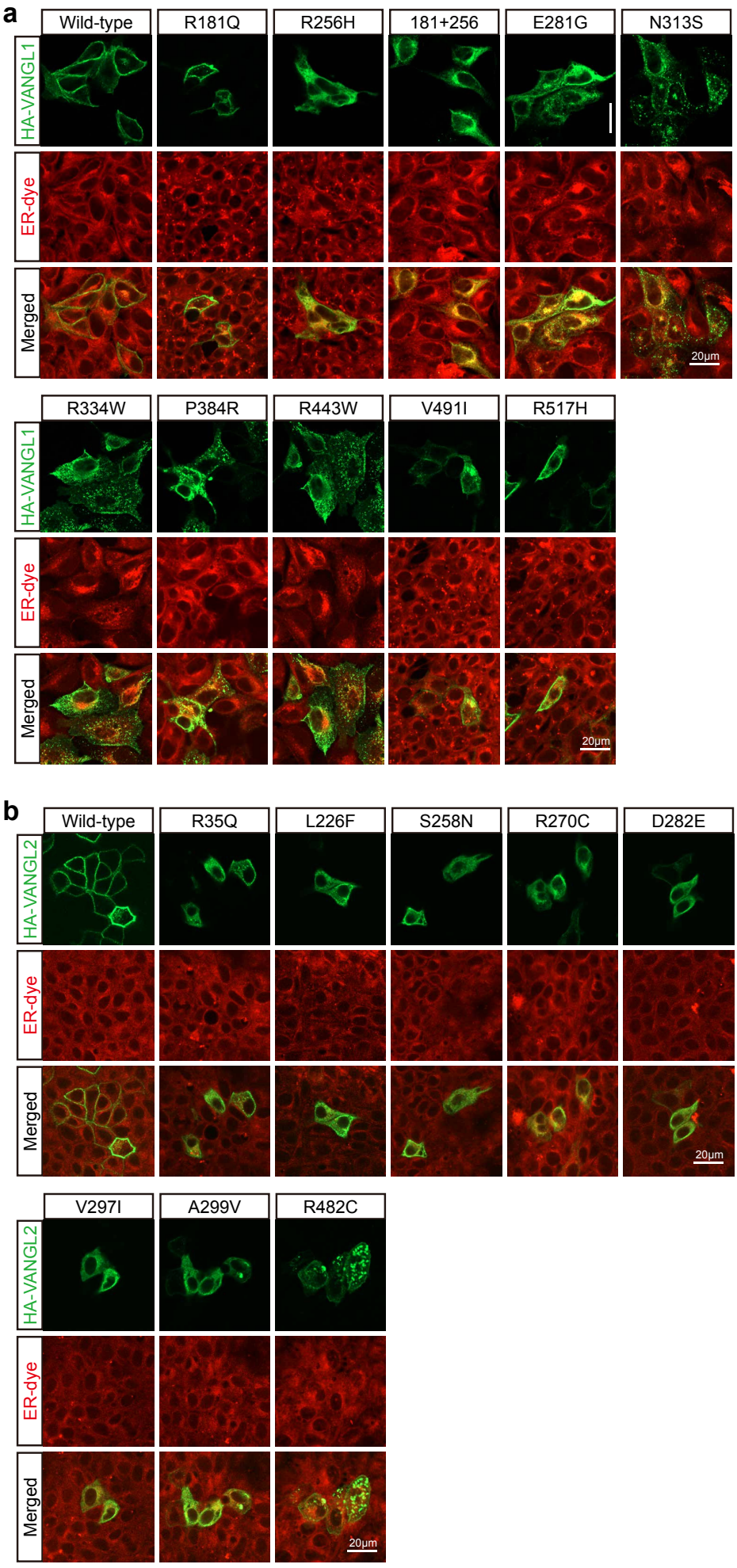

Figure S7. The intracellular localization of VANGL1 and VANGL2 variants. The HA-tagged wildtype and mutant VANGL1/2 proteins were stained in green and the ER was visualized by ER-dye in red.

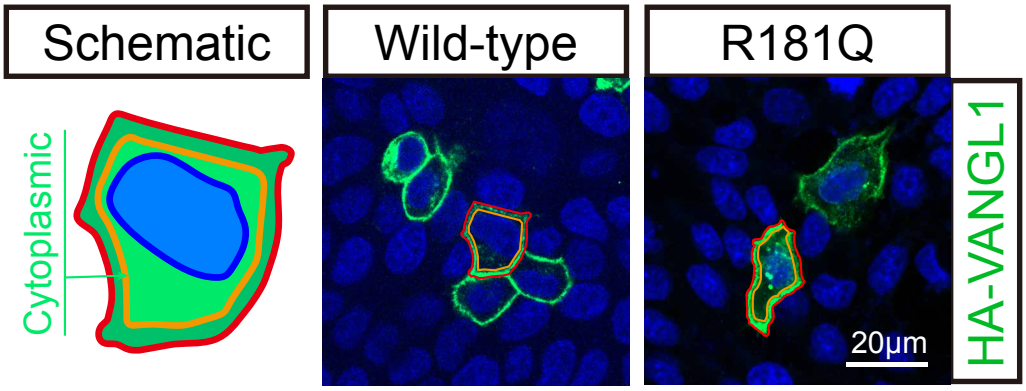

$$\text{Membrane ratio} = \frac{\text{Total integrated density} - \text{Intracellular density}}{\text{Total integrated density}}$$

Figure S8. A schematic of membrane to total ratio of quantification of membrane localization. Membrane ratio = (Total integrated density [Red] - Intracellular density [Yellow]) / Total integrated density [Red].

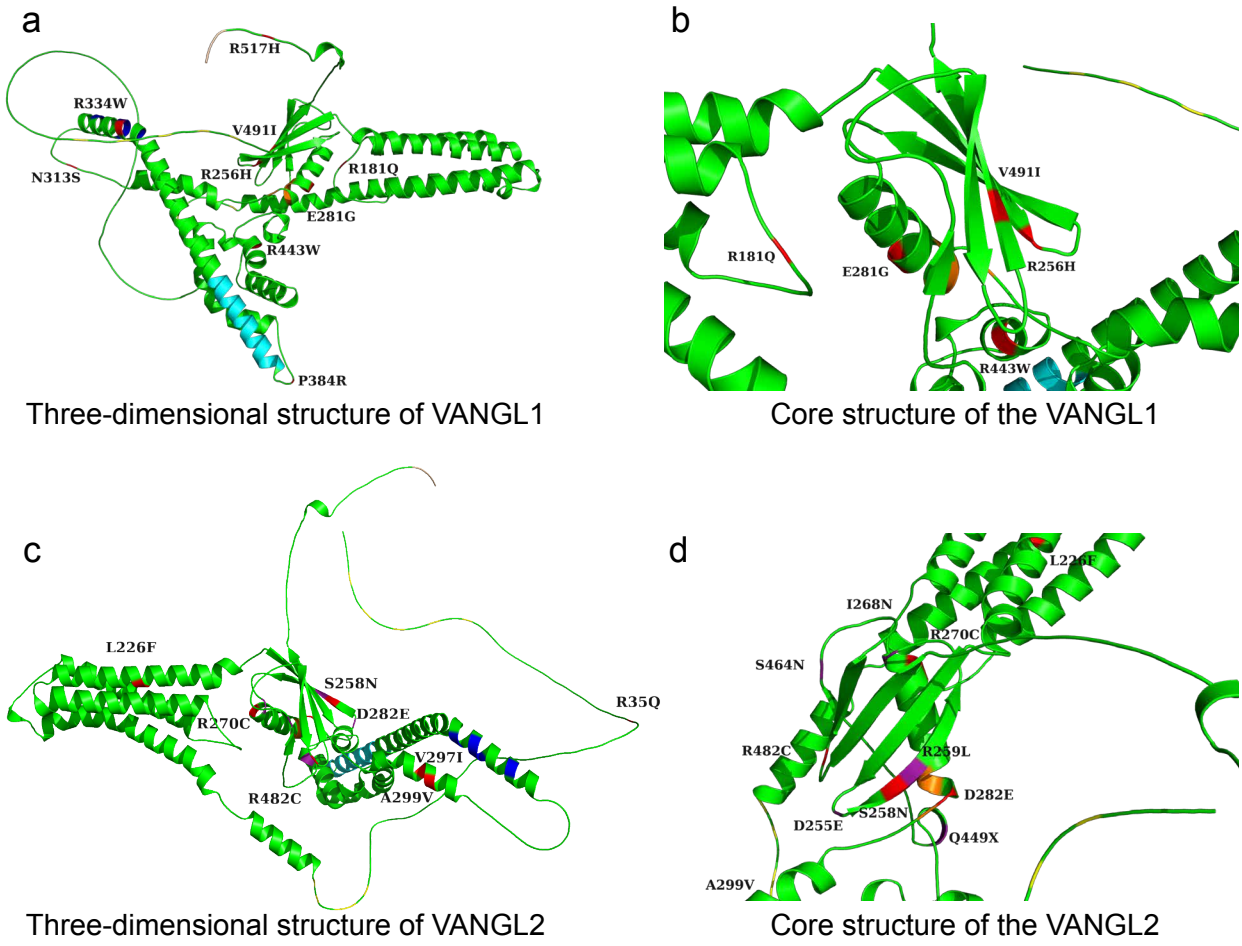

Figure S9. The 3D structures of VANGL1 and VANGL2 predicted by AlphaFold. The models of VANGL1 (Q8TAA9) and VANGL2 (Q9ULK5) were built by AlphaFold (https://alphafold.ebi.ac.uk/). The structures of VANGL1/2 and distribution of variants were presented by PyMOL software (https://pymol.org/2/). Three *VANGL1* variants (p.R256H, p.E281G, and p.V491I) an four *VANGL2* variants (p.S258N, p.R270C, p.D282E, and p.R482C) are located within the core structure of the protein. Red: VANGL variants found in our multicenter cohort; yellow: two highly conserved phosphorylation clusters; orange: trans-Golgi network; blue: p97/valosin-containing protein (VCP)-interacting motif; light blue: coiled-coil domain; wheat: PDZ binding motif.

Table S1. Clinical and radiographic characterics of subjects with *VANGL1* or *VANGL2* variants

Case	HK0001	SCO2003P0130	SCO2003P0531	SCO2003P1220	SCO2003P1319	SCO2003P1232	SCO1906P0098	SCO2003P2246	SCO1908P0074	SCO2003P1178	SCO2003P0196	SCO1908P0163	SCO2003P0613	US0001[a]	US0002[b]	JP0001	SCO2003P0386	SCO2003P0525	SCO2105P3029
Disease gene	*VANGL1*	*VANGL1*	*VANGL1*	*VANGL1*	*VANGL1*	*VANGL1*	*VANGL1*	*VANGL1*	*VANGL1*	*VANGL1*	*VANGL1*	*VANGL2*	*VANGL2*	*VANGL2*	*VANGL2*	*VANGL2*	*VANGL2*	*VANGL2*	*VANGL2*
Variant	c. 542G>A +c.767G>A	c.842A>G	c.938A>G	c.938A>G	c.938A>G	c.1000C>T	c.1151C>G	c.1151C>G	c.1327C>T	c.1471G>A	c.1550G>A	c.104G>A	c.676C>T	c.773G>A	c.808C>T	c.846C>A	c.889G>A	c.896C>T	c.1444C>T
Age (year)	16	5	19	15	5	4	2	44	3	7	16	5	2	NA	NA	NA	14	17	16
Sex	M	M	F	M	F	M	M	M	F	M	M	M	M	M	NA	NA	M	M	F
Height (cm)	177	97	150	168	NA	103	NA	158	97	115	158	115	85	NA	NA	NA	160	155	NA
Weight (kg)	59.4	NA	54	45	NA	NA	NA	69	16	NA	55	NA	13	NA	NA	NA	46	43	NA
Skeletal abnormalities																			
Scoliosis	+	+	+	+	+	+	+	+	+	+	+	+	+	+	+	+	+	+	+
Vertebral malformations	C7-T1 NSH	T4-T12, L2 SD; L1 NSH	L1 SW	L4, L5 NSW	T3-T5 SD	T10, T12 SH	T1, T2 SH	C5, T5, L3 NSH; T6 NSB; C4-C7, T4-T7, L3-L5 SD	L2-L3 NSH	T10-L2 SD; L1 NSH	T9, T11 NSB; T10 NSW; T12 NSH; L1 SD	T12 SH	T10 SB; T9, T11 FF	SH	VACTEL	T11 SH	L2 SH	T6-10 SD, T8 SW	T9 SB, T12 SH
Scoliosis classification	III	III	I	III	II	I	I	III	III	III	III	I	I	NA	NA	I	I	III	I
Max Cobb	21.7	72	55	47	50	56	72	46	25	108	135	34	42.5	NA	NA	40	58	70	44
Rib malformations	R13 N-R	R8-12 F-R	-	-	-	R10 L-L	-	-	-	-	R11 L-R	R12 L-R	R1 L-R	-	-	-	-	-	-
Other system abnormalities																			
Neurologic	-	DM, SM, SB, ISC	TSH, DM, SB, DS	SM	-	SS	SM	-	-	DM, TSH, SS, DS	TSH, DM, DS	SS	SB	-	-	-	SS, TSH	SB	TSH
Cardiovascular	-	-	-	-	-	-	-	AI	-	-	-	-	-	VSD	VSD	-	-	-	-
Pulmonary	-	-	-	-	-	-	-	-	-	-	-	-	-	-	TE fistula	-	-	Restrictive ventilation	-
Ocular	-	-	-	-	-	-	-	-	-	-	-	-	-	-	-	-	-	-	-
Digestive	-	Splenomegaly	-	-	-	-	-	-	-	-	-	-	-	-	TE fistula	-	-	-	-
Urinary	-	-	-	-	-	-	-	Horseshoe kidney	-	-	-	-	-	-	-	-	-	-	-
Reproductive	-	-	-	-	-	-	-	-	-	-	-	-	-	-	-	-	-	-	-
Others	-	-	Club foot	-	Cleft palate	Nephritis	Unilateral thyroid	-	-	-	-	Preterm baby	Inguinal hernia	Cleft palate, facial dysmorphia, and ear abnormalities	-	-	Appendicitis	Chest deformity	-

NA, not available; T, thoracic vertebra; L, lumbar vertebra; R, rib; SD, segmentation defect; SH, segmented hemivertebra; NSH, non-segmented hemivertebra; SW, segmented wedged vertebra; NSW, non-segmented wedged vertebra; NSB, non-segmented butterfly vertebra; FF, failure of formation; N-R, additional rib at right side; L-L, absent rib at left side; L-R, absent rib at right side; F-R, fused rib at right side; SM, syringomyelia; DM, diastematomyelia; TSH, tethered spinal cord; SS, sacral schisis; ISC, intraspinal cyst; SB, spinal bifida, DS, dermal sinus; AI, aortic insufficiency; VSD, ventral septal defect; TE, tracheoesophageal. [a]Patient was diagnosed with hemifacial microsomia, Goldenhar syndrome (also known as oculo-auriculo-vertebral spectrum disorder) with hemivertebrae, facial dysmorphia (facial asymmetry, small half of face,malar hypoplasia, mandibular hypoplasia, micrognathia), and ear abnormalities (external ear deformity, external auditory canal atresia, microtia, hearing loss). [b]Patient was diagnosed with VACTERL (Vertebral abnormalities, anal atresia, cardiac defects, tracheal anomalies, esophageal atresia, renal and radial abnormalities, and limb abnormalities) syndrome.

Table S2. Comparison of clinical features of subjects with or without *VANGL1/2* mutations in the Beijing cohort

Variable	Overall	Non-*VANGL*	*VANGL*	P-Value
Number of subject, n	708	693	15	
Age of onset, mean (SD)	5.0 (5.6)	5.1 (5.6)	4.0 (5.6)	0.478
Gender, n (%)				
Female	367 (51.8)	363 (52.4)	4 (26.7)	0.087
Male	341 (48.2)	330 (47.6)	11 (73.3)	
Scoliosis classification*, n (%)				
I	233 (32.9)	227 (32.8)	6 (40.0)	0.680
II	96 (13.6)	95 (13.7)	1 (6.7)	
III	379 (53.5)	371 (53.5)	8 (53.3)	
Spinal curvature number, mean (SD)	1.5 (0.8)	1.5 (0.8)	1.8 (0.9)	0.230
Max cobb, mean (SD)	59.9 (26.4)	59.8 (26.4)	61.0 (28.4)	0.880
Max cobb classification, n (%)				
Mild (10-30°)	51 (7.2)	50 (7.2)	1 (6.7)	0.882
Moderate (30-45°)	179 (25.3)	176 (25.4)	3 (20.0)	
Severe (> 45°)	478 (67.5)	467 (67.4)	11 (73.3)	
Intraspinal deformity, n (%)				
No	502 (70.9)	499 (72.0)	3 (20.0)	<0.001
Yes	206 (29.1)	194 (28.0)	12 (80.0)	
Rib malformation, n (%)				
No	465 (65.7)	455 (65.7)	10 (66.7)	0.847
Yes	243 (34.3)	238 (34.3)	5 (33.3)	
Cardiovascular defect, n (%)				
No	617 (87.1)	603 (87.0)	14 (93.3)	0.707
Yes	91 (12.9)	90 (13.0)	1 (6.7)	
Ocular defect, n (%)				
No	700 (98.9)	685 (98.8)	15 (100.0)	1.000
Yes	8 (1.1)	8 (1.2)	0 (0.0)	
Digestive defect, n (%)				
No	662 (93.5)	648 (93.5)	14 (93.3)	1.000
Yes	46 (6.5)	45 (6.5)	1 (6.7)	
Urinary defect, n (%)				
No	650 (91.8)	636 (91.8)	14 (93.3)	1.000
Yes	58 (8.2)	57 (8.2)	1 (6.7)	
Reproductive defect, n (%)				
No	700 (98.9)	685 (98.8)	15 (100.0)	1.000
Yes	8 (1.1)	8 (1.2)	0 (0.0)	

*Classification was based on anatomic location and type of anomaly. Three types of defects (I, II, III) were denoted as failure of formation, failure of segmentation, or mixed type, respectively.

Deciphering disorders Involving Scoliosis and COmorbidities (DISCO) study

Guixing Qiu[1, 2, 3, 4], Nan Wu[1, 2, 3, 4], Jianguo Zhang[1, 2, 3, 4], Zhihong Wu[2, 3, 4, 5], Shengru Wang[1, 3, 4], Sen Liu[1, 3, 4], Ziquan Li[1, 3, 4], Yang Yang[1, 3, 4], Zhengye Zhao[1, 3, 4], Guilin Chen[1, 3, 4], Guozhuang Li[1, 3, 4], Yuanpeng Zhu[1, 3, 4], Jihao Cai[1, 3, 4], Di Liu[1, 3, 4], Kexin Xu[1, 3, 4], Jianle Yang[1, 3, 4], Aoran Maheshati[1, 3, 4], Qing Li[1, 3, 4], Jingyi Xie[1, 3, 4], Xiangjie Yin[1, 3, 4], Jie Wang[1, 3, 4], Zihua Li[1, 3, 4], Zhifa Zheng[1, 3, 4], Kun Fang[1], Xiangyu Nie[1], Xi Cheng[1], Wen Wen[1], Xinyu Yang[6], Yuanqiang Zhang[6], Lian Liu[6], Lianlei Wang[6], Na Chen[7], Jiachen Lin[8], Mao Lin[8], Lina Zhao[1, 3, 5], Fei Liu[1, 3, 5], Yuchen Niu[9], Qing Liu[1], Guangxi Gao[1], Shuai Li[1], Yueyan Bai[1], Sen Zhao[10], Yongyu Ye[11], Hengqiang Zhao[12], Zefu Chen[13], Jiaqi Liu[14], Zihui Yan[15], Chenxi Yu[16], Jiashen Shao[17]

1. Department of Orthopedic Surgery, Peking Union Medical College Hospital, Peking Union Medical College and Chinese Academy of Medical Sciences, Beijing, 100730, China.
2. State Key Laboratory of Complex Severe and Rare Diseases, Peking Union Medical College Hospital, Peking Union Medical College and Chinese Academy of Medical Sciences, Beijing, 100730, China.
3. Beijing Key Laboratory for Genetic Research of Skeletal Deformity, Beijing, 100730, China.
4. Key Laboratory of Big Data for Spinal Deformities, Chinese Academy of Medical Sciences, Beijing, 100730, China.
5. Medical Research Center, Peking Union Medical College Hospital, Peking Union Medical College and Chinese Academy of Medical Sciences, Beijing, 100730, China.
6. Department of Orthopaedic Surgery, Qilu Hospital, Cheeloo College of Medicine, Shandong University, Jinan, 250012, China.
7. Department of Obstetrics and Gynaecology, Peking Union Medical College Hospital, Peking Union Medical College and Chinese Academy of Medical Sciences, Beijing, 100730, China.
8. Department of Orthopedics, The First Affiliated Hospital, Zhejiang University School of Medicine, Zhejiang, 310006, China.
9. Clinical Biobank, Medical Research Center, National Science and Technology Key Infrastructure on Translational Medicine, Peking Union Medical College Hospital, Chinese Academy of Medical Sciences and Peking Union Medical College, Beijing, 100730, China.

10. Department of Molecular and Human Genetics, Baylor College of Medicine, Houston, TX 77030, USA.
11. Department of Orthopedic Surgery, Guangdong Provincial People's Hospital, Southern Medical University, Guangzhou, 510080, China.
12. Feinberg School of Medicine, Northwestern University, Chicago, IL 60611, USA.
13. Division of Spine Surgery, Department of Orthopedics, Nanfang Hospital, Southern Medical University, Guangzhou, 510515, China.
14. Department of Breast Surgical Oncology, Cancer Hospital Chinese Academy of Medical Sciences, Beijing, 100021, China.
15. Chinese Academy of Medical Sciences, Peking Union Medical College, Beijing, 100730, China.
16. Department of Orthopedics, Shandong Provincial Hospital, Shandong First Medical University, Shandong, 250021, China.
17. Department of Orthopedics, Beijing Friendship Hospital, Capital Medical University, Beijing, 100050, China.

Japanese Early Onset Scoliosis Research Group

Nao Otomo[1, 2], Yoshiro Yonezawa[1, 2], Kazuki Takeda[1, 2], Yoji Ogura[1], Noriaki Kawakami[3], Toshiaki Koatani[4], Teppei Suzuki[5], Koki Uno[5], Hideki Sudo[6], Satoshi Inami[7], Hiroshi Taneichi[7], Hideki Shigematsu[8], Kei Watanabe[9], Ryo Sugawara[10], Yuki Taniguchi[11], Shohei Minami[4], Masaya Nakamura[1], Morio Matsumoto[1], Shiro Ikegawa[2], Kota Watanabe[1]

1. Department of Orthopedic Surgery, Keio University School of Medicine, Tokyo, 160-8582, Japan
2. Laboratory of Bone and Joint Diseases, RIKEN Center for Integrative Medical Sciences, Tokyo, 108-8639, Japan
3. Department of Orthopaedic Surgery, Meijo Hospital, Nagoya, 460-0001, Japan
4. Department of Orthopaedic Surgery, Seirei Sakura Citizen Hospital, Sakura, 285-8765, Japan
5. Department of Orthopaedic Surgery, National Hospital Organization, Kobe Medical Center, Kobe, 654-0155, Japan
6. Department of Advanced Medicine for Spine and Spinal Cord Disorders, Hokkaido University Graduate School of Medicine, Sapporo, 060-8638, Japan
7. Department of Orthopaedic Surgery, Dokkyo Medical University School of Medicine, Mibu, 321-0293, Japan
8. Department of Orthopaedic Surgery, Nara Medical University, Kashihara, 634-8522, Japan
9. Department of Orthopaedic Surgery, Niigata University Hospital, Niigata, 951-8520, Japan
10. Department of Orthopaedic Surgery, Jichi Medical University, Shimotsuke, 329-0498, Japan
11. Department of Orthopaedic Surgery, Faculty of Medicine, The University of Tokyo, Tokyo, 113-8655, Japan